Weldability of Fe_3Al-Type Aluminide

Although still sensitive to minor shifts in alloy composition, the weldability of iron aluminides shows promise with the electron beam process

BY S. A. DAVID AND T. ZACHARIA

ABSTRACT. An investigation was carried out to determine the weldability of a series of Fe_3Al-type alloys. Autogenous welds were made on thin sheets of iron aluminide alloys using gas tungsten arc (GTA) and electron beam (EB) welding processes at different travel speeds and power levels. The results indicate that although these alloys can be successfully welded using the EB welding process, some compositions may hot crack during GTA welding. Boron and zirconium additions have been found to promote hot cracking in these alloys. Among the alloys investigated, Fe_3Al modified with chromium, niobium and carbon (FA-129) showed the most promise for good weldability. Hot-cracking severity of this alloy was further investigated using the Sigmajig test. The minimum threshold stress of 25 ksi measured is within the material range of other aluminides and some commercial stainless steels. Also, some of these alloys exhibited a tendency for cold cracking. This is related to severe hydrogen embrittlement associated with this class of alloys.

Introduction

Recently, considerable interest has been generated in the ordered intermetallic alloys because of their unique properties, such as yield strength that increases with temperature, and oxidation and corrosion resistance that make them attractive for high-temperature structural applications (Refs. 1–7). Although the potential of intermetallic alloys has been known for some time, their tendency to be brittle has limited their use for structural applications. Generally, brittleness in an alloy can be attributed to one of the two major factors, *viz.*, insufficient number of slip systems (Ref. 8) or grain-boundary weakness (Refs. 9, 10). Ordered alloys with low-crystal symmetries do not offer enough slip systems to permit extensive deformation. Examples include Co_3V, Ni_3V, Ti_3Al, etc. In other alloys such as Ni_3Al, adequate deformation modes may exist and yet the alloy may have grain boundaries that are inherently weak. The renewed interest in these alloys is a result of work at several laboratories showing that ductility and fabricability of several intermetallic alloys can be substantially improved using physical metallurgy principles such as microalloying for grain-boundary strength and macroalloying for changing the crystal structure to maximize the number of slip systems (Refs. 6, 7, 11, 12).

One of the major considerations in developing ductile intermetallic alloys for structural applications is weldability, *i.e.*, the ease with which the alloys can be welded or joined. Since these alloys achieve their unique properties from their ordered crystal structure, the behavior during a weld thermal cycle is very critical. Weldability has been found to be a strong function of composition and welding parameters (Refs. 13–17). Solidification behavior, atomic mobility, ordering kinetics, and the resulting mechanical behavior can influence the weldability and properties to a great extent.

An alloy of recent interest in this class of materials is the iron-aluminide (Fe_3Al type). Although interest in this particular alloy dates back to the 1930s (Refs. 18, 19), recent renewed interest stems from its unique properties and advantages, such as excellent oxidation resistance, better strength-to-weight ratio compared to stainless steels, low-cost raw materials, and, finally, conservation of strategic elements. However, lack of ductility at room temperature and sharp reduction in strength above 600°C (1112°F) are major obstacles in its utilization as structural materials. Recent studies have shown that adequate ductility can be achieved in these alloys through control of composition and microstructure (Refs. 20–23). Binary Fe_3Al alloy compositions have been modified by macroalloy additions (< 10%) and microalloy additions (< 1%) (Ref. 24). These additions have been found to improve the fabricability and aqueous corrosion resistance of these alloys. Zirconium and niobium have been found to form boride and carbide precipitates, respectively, that strengthen these alloys, refine the grain structure, and increase recrystallization temperature (Ref. 25). Chromium improves the room-temperature ductility.

KEY WORDS

Weldability Testing
Fe_3Al-Type Aluminide
Autogenous Welds
GTAW
Electron Beam Weld
Hot Cracking
Cold Cracking
Threshold Stresses
Sigmajig Testing
Intermetallic Alloys

S. A. DAVID and T. ZACHARIA are with Oak Ridge National Laboratory, Metals and Ceramics Division, Oak Ridge, Tenn.

Table 1 — Alloy Composition (wt-%)

Heat	Al	Cr	Nb	Zr	B	C	Fe
FA-122B	15.88	5.46	—	0.19	0.01	—	Bal.
FA-124B	15.89	5.47	—	—	0.01	—	Bal.
FA-127B	15.83	5.44	0.97	—	—	—	Bal.
FA-129B	15.86	5.45	0.97	—	—	0.05	Bal.

An earlier investigation of the weldability of Fe_3Al-type alloys showed that the weldability is very sensitive to the welding conditions and composition, producing good welds sometimes and severely cracked welds at other times (Ref. 16). This paper addresses the preliminary weldability studies and weld microstructures of advanced Fe_3Al alloys recently developed at Oak Ridge National Laboratory (ORNL) (Ref. 23).

Experimental Procedure

The alloys used in this study are listed in Table 1. The alloys were prepared by arc melting under argon and drop casting into a water-cooled copper mold. The alloy castings were hot rolled to a final thickness of 0.76 mm (0.03 in.) starting at 1000°C (1832°F) and finishing at 650°C (1202°F). Two thermomechanical processing conditions were utilized to optimize the properties of the alloys: 1) the alloy finished to the final thickness by hot rolling at 650°C (designated B); and 2) hot rolled at 650°C followed by an anneal at 750°C (1382°F) for 1 h and subsequent oil quench (designated BQ). The microstructure of the hot-rolled material contained predominantly elongated grains. However, annealing the hot-rolled alloy for 1 h resulted in recrystallized grain structure as shown in Fig. 1. The welding variables were adjusted to produce full-penetration welds at various welding speeds ranging from 2.1 to 21.2 mm/s (5 to 50 in./min) for electron beam (EB) welds and 4.2 to 25.4 mm/s (10 to 60 in./min) for gas tungsten arc (GTA) welds. Both EB and GTA welds were made on 20 X 40 X 0.7-mm (0.8 X 1.6 X 0.03-in.) coupons. Welding parameters used to produce full-penetration EB welds were: accelerating voltage 75 kV and beam current 1.7 to 5.6 mA; and for GTA welds: welding voltage of 9.5 V and welding current of 35 to 75 A. For the range of welding speeds investigated, the linear heat input for GTA welds ranged from 63 J/mm at the slowest welding speed to 22 J/mm at the highest welding speed. Similarly, the linear heat input for EB welding ranged from 48 to 15 J/mm. The calculation of heat input utilized an efficiency value of 80% for both processes.

The susceptibility to fusion zone (FZ) solidification cracking was determined using the Sigmajig test (Ref. 26). The test evaluates the hot-cracking tendency of the alloy using the GTA welding process. The test ranks materials by quantitatively measuring the threshold stress (σ_o) above which cracking in the FZ occurs during welding. Sigmajig tests were performed using the GTA welding process on 0.7-mm-thick sheet material of the alloys using 70-A DC electrode negative polarity, at 12.5 mm/s travel (30 in./min) and 1-mm arc length. Microstructural characterization was performed using conventional metallographic techniques. The specimens for light microscopy were etched with a solution containing 40 mL HNO_3, 60 ml CH_3COOH, and 20 mL HC1.

Results and Discussion

Electron Beam Welding

Previous investigation on the weldability of ordered intermetallic alloys has shown that the high-energy beam process, in general, can produce successful welds owing to the highly concentrated heat source and possible refinement in the FZ structure (Ref. 14). However, recent weldability studies (Ref. 16) have shown that the iron aluminide alloys, although weldable at low welding speeds using EB, tend to crack severely with increasing welding speed. The observed increase in cracking was attributed to the high heating and cooling rates and the associated steep thermal gradients and stresses that develop within the FZ and the heat-affected zone (HAZ). The various Fe_3Al alloys were EB welded at speeds ranging from 2.1 to 21.2 mm/s. After welding, the specimens were carefully examined for cracks using a low-magnification microscope. There were no observable cracks in any of the EB welds for the four alloys investigated at a magnification of 10X under light microscopy. The results of EB welding of Fe_3Al-type alloys in both conditions indicate that successful full-penetration EB welds can be made in thin sheets for the range of welding speeds investigated. In general, the preliminary results suggest that these Fe_3Al-type alloys may be autogenously welded using the EB process. It was surprising that even the alloys containing boron (FA-122B and FA-124B) did not show any tendencies to hot crack. From previous experiences on aluminides, in particular iron alu-

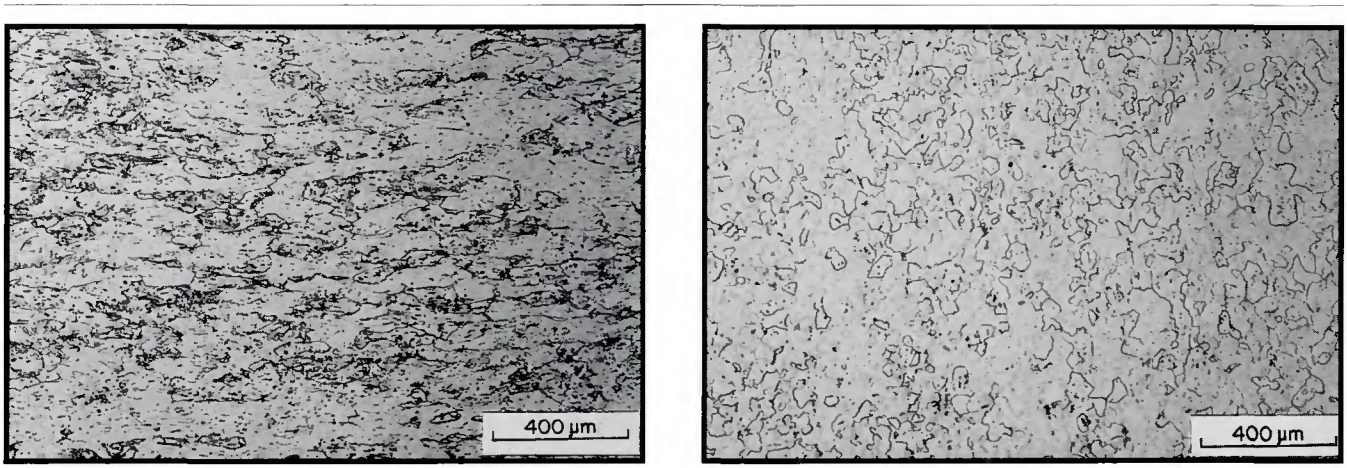

A B

Fig. 1 — Optical photomicrographs of alloy FA-129. A — Microstructure of the hot rolled alloy; B — microstructure of the hot rolled alloy after 1 h anneal at 750°C.

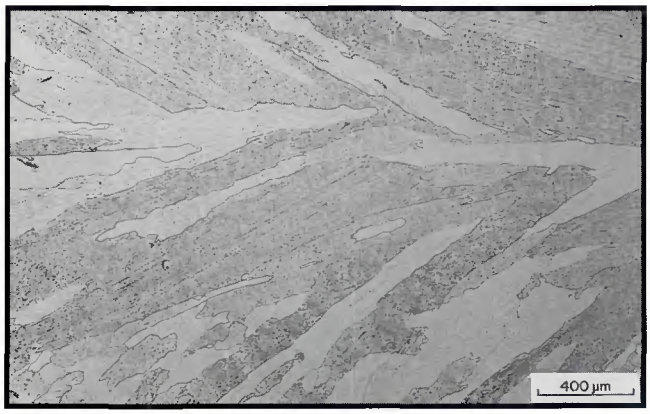

A

B

Fig. 2 — Optical photomicrographs. A — Surface; B — transverse sections of FA-129B electron beam weld (2.1 mm/s).

minides, boron has been found to be detrimental for weldability (Ref. 16). Perhaps the absence of any hot cracks during EB welding of these alloys can be attributed to the refined microstructural features.

Hot cracking has been the subject of extensive studies (Refs. 27–30). Different manifestations of hot cracking during welding are:

1) solidification cracking
2) liquation cracking in the HAZ
3) a combination of the above two
4) elevated-temperature (sub-solidus) cracking during heat treatment of the weld.

Several theories have been proposed to explain the mechanism of hot cracking (Refs. 31–35). Solidification cracking in weld metal often occurs during later stages of solidification when the strains resulting from thermal and solidification contraction exceed the ductility of the partially solidified metal. Solidification cracking has been known to be favored by the factors that decrease the solid-solid contact area during the last stages of solidification. Two of the most important factors are low-melting segregates and grain size. Low-melting segregates at the grain boundaries may exist as a liquid film to temperatures well below the equilibrium solidus and reduce the grain-boundary contact area to a minimum (Ref. 36). Liquid pools trapped between the grains or interdendritic regions greatly influence the tensile properties of the partially solidified alloy. Also, the coarser the grain structure, the less the grain-boundary contact areas for a given amount of nonequilibrium liquid. Hence, coarse-grained FZ structures are generally more prone to solidification cracking than fine-grained ones. Also, the mechanical behavior of the partially solidified alloy determines its solidification cracking sensitivity. Since all alloys do not hot crack, it is clear that some liquid plus solid microstructures are more susceptible to hotcracking than others, stresses being equal. The study did not attempt to measure the mechanical behavior of the material at temperatures exceeding the solidus temperature.

The absence of hot cracks during EB welding of the iron aluminide alloys investigated here may be attributed to the fine-grain FZ structure. The formation of fine-grain FZ structure in these welds is explained below. Regarding the HAZ liquation cracking, results of this investigation, as well as the past experience (Ref. 16), indicate that iron-aluminide alloys are not prone to HAZ cracking.

Figures 2 and 3 show typical photomicrographs of the FA-129B alloy EB welds made at 2.1 mm/s and 21.2 mm/s, respectively. The low-speed weld contains predominantly coarse columnar grains, and the high-speed weld contains fine fusion zone grain structure. In addition, there is clear evidence of extensive recrystallization and grain growth occurring in the HAZ. This may have significant implications regarding the grain structure of the FZ. Commonly, the weld-metal or FZ grain structure is predominantly determined by the base-metal grain structure and the welding conditions. The base metal acts as an ideal substrate on which solidification proceeds. Initial growth occurs epitaxially at the partially melted grains in the base metal. Since the base metal used for welding in this study does not appear to have gone through a complete recrystallization and/or grain growth (textured structure is still evident), *in situ* recrystallization and the formation of a number of grains at the

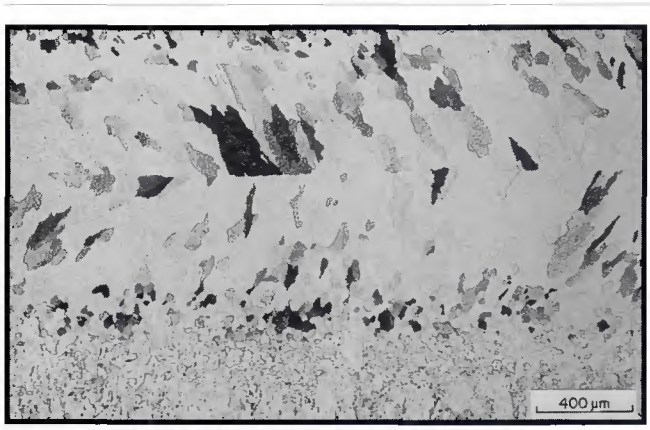

A

B

Fig. 3 — Optical photomicrographs. A — Surface; B — transverse sections of FA-129B electron beam weld (21.2 mm/s).

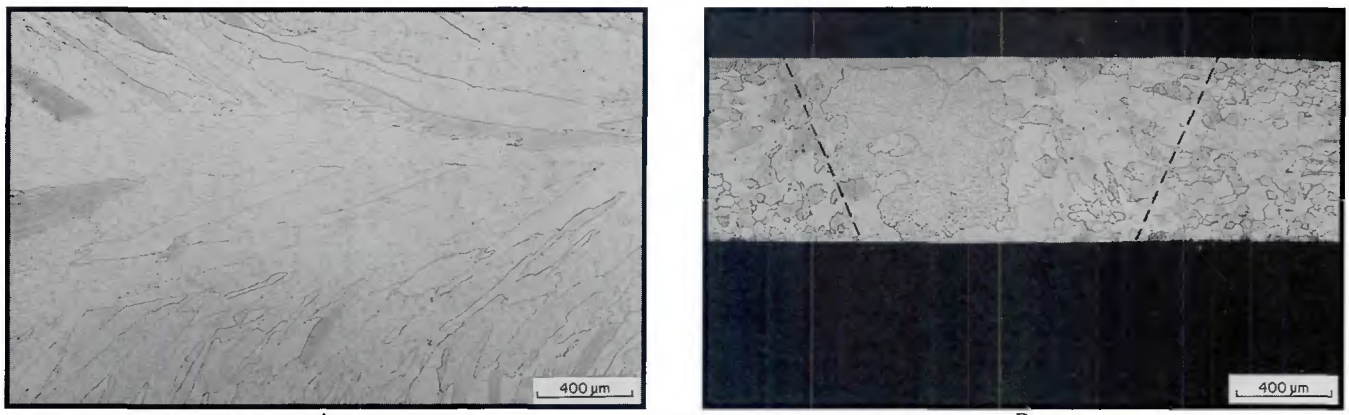

A B

Fig. 4 — Optical photomicrographs. A — Surface; B — transverse sections of FA-122B electron beam weld (2.1 mm/s).

fusion line may promote a finer FZ grain structure. Therefore, in this study, the grain structure of the FZ depends to a large extent on the welding parameters and the extent of recrystallization that occurs at the fusion line.

Figures 4 and 5 show typical photomicrographs of the FA-122B alloy EB welds made at 2.1 mm/s and 21.2 mm/s, respectively. The analysis of these photomicrographs also reveals extensive recrystallization in the HAZ. The FZ microstructure was finer for the high-speed weld than for the low-speed weld for the reasons described above. No significant difference was found in the welding behavior or microstructural characteristics between the welds made on hot-rolled and hot-rolled plus oil-quenched initial conditions. Figure 6 shows typical photomicrographs of EB welds made on FA-129 alloy in the BQ condition. The FZ microstructure appears very similar to that of the welds made on FA-129B in the as-rolled condition. The HAZ, however, shows evidence of significant grain growth. The recrystallized base metal structure of the FA-129BQ alloy resulted in larger grains near the fusion line after exposure to the weld thermal cycle.

Gas Tungsten Arc Welding

Table 2 summarizes the results of the GTA welding of Fe_3Al as a function of welding speed for the different alloys considered in this investigation. Full-penetration GTA welds were made at welding speeds ranging from 4.2 to 25.4 mm/s. After welding, the specimens were carefully examined for cracks using a low magnification (10X) microscope. The results indicated that some of the alloys can be successfully welded using the GTA welding process at low welding speeds. All of the alloys exhibited a tendency to crack at the highest welding speed of 25.4 mm/s. Among the four alloys, FA-122B (containing zirconium and boron) cracked severely at all welding speeds investigated. Zirconium and boron may be detrimental for the weldability of this alloy. The other alloys (FA-124B, FA127B, and 129B) exhibited a tendency to crack only at the highest welding speed. The initial condition of the alloy did not have any major influence on the cracking sensitivity of the alloy. Based on previous experience (Ref. 16), the hot-cracking behavior of these alloys during GTA welding is no surprise. The hot-cracking tendency of some of these alloys, in particular the ones containing boron and zirconium, can be attributed to the presence of low-melting liquid and its distribution during the last stages of solidification. Among these alloys, the niobium modified alloy (FA-129) showed the most promise for good weldability. From Tables 1 and 2, it is evident that zirconium in combination with boron produces cracking at all welding speeds. However, FA-129B alloy did not show any cracking tendencies except at the highest welding speed. It must be noted that the high welding speeds were chosen to produce conditions that could promote cracking in a crack-sensitive alloy.

Figure 7 shows typical photomicrographs of alloy FA-129B GTA welds. The FZ grain structure is rather coarse and columnar because of the higher heat input compared to the EB welds. As in the EB welds, extensive recrystallization had taken place in the HAZ. Because of the higher heat input involved in the process, subsequent to recrystallization, grain growth had also taken place. Therefore, the HAZ grain structure was coarser than the one observed in EB

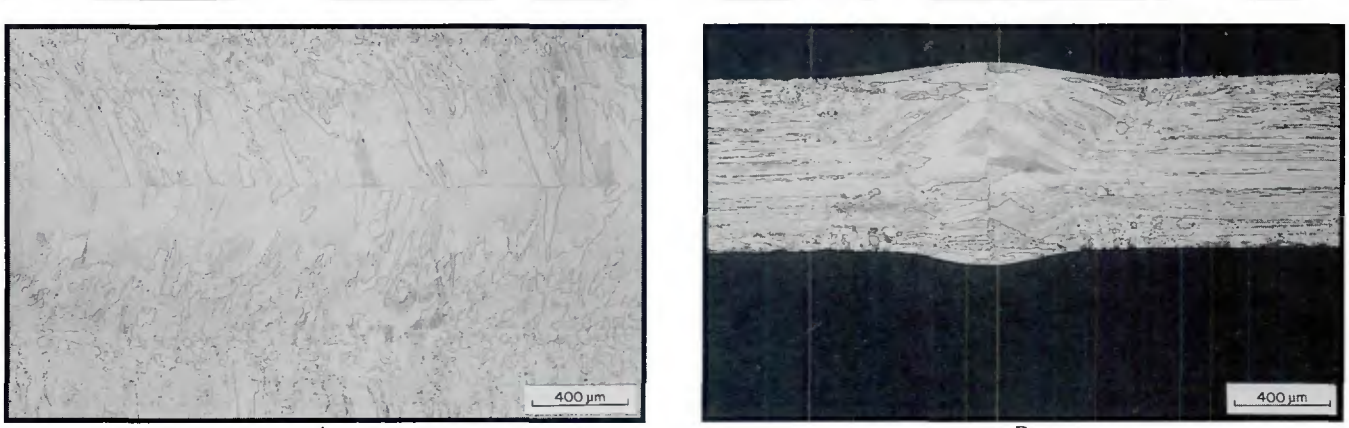

A B

Fig. 5 — Optical photomicrographs. A — Surface; B — transverse sections of FA-122B electron beam weld (21.2 mm/s).

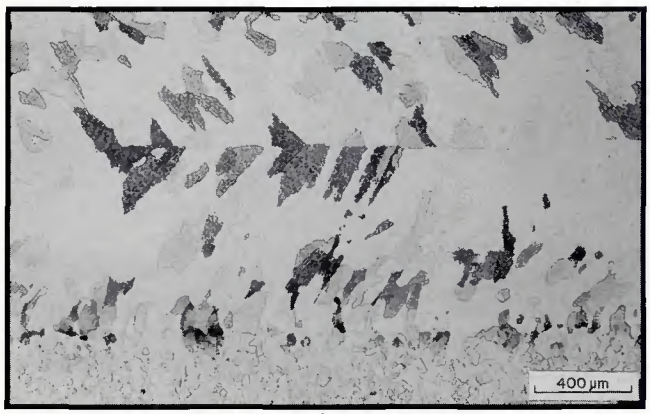

A

B

Fig. 6 — Optical photomicrographs. A — Surface; B — transverse sections of alloy FA-129BQ electron beam weld (21.2 mm/s).

welds. Figure 8 shows typical photomicrographs of alloy FA-122B GTA welds with centerline hot cracks, which show the extreme sensitivity of this alloy for hot cracking. As pointed out earlier, the alloy and the microstructure have been rendered sensitive to hot cracking by the presence of boron and zirconium in the alloy. Figure 9 shows a scanning electron microscope (SEM) photomicrograph of the centerline crack in the FZ. The fracture surface of the specimen exhibits dendritic features typical of a hot crack or solidification crack.

Hydrogen Cracking

Although crack-free GTA welds were produced in FA-129 alloy, the weldment showed evidence of cold cracking or delayed cracking subsequent to welding. A typical cold crack in the weldment is shown in Fig. 10. This type of cracking is typical of either the HAZ or the FZ of low-alloy and other hardenable steels, and it is associated with hydrogen embrittlement. Recent studies by Liu and coworkers at ORNL indicate that Fe_3Al-type alloys are susceptible to environmental embrittlement at room temperature in which atomic hydrogen is the embrittling agent (Ref. 37). Their results showed that water vapor in the atmosphere reacts with aluminum to form alumina and atomic hydrogen. The atomic hydrogen diffuses into the metal along cleavage planes and causes embrittlement. Figure 11 shows an SEM photomicrograph of a typical cold-cracked surface of the FA-129BQ alloy weldment, indicating cleavage fracture.

The basic requirements for cold cracking or delayed cracking are sufficient hydrogen levels, a susceptible microstructure, and tensile stresses in the weldment. During welding, hydrogen in the form of water vapor is carried to the arc atmosphere by the shielding gas, or surface contamination. This hydrogen is converted to the atomic state and readily dissolves in the weld metal. (This could perhaps explain the absence of cracks in EB welds made on FA-129B, owing to the controlled atmosphere in the vacuum chamber.) Further, during welding, sufficient stresses are present due to the generation of thermal stress and solidification stresses under restrained conditions. All of these factors seem to have contributed to the observed cold-cracking behavior in Fe_3Al-type alloys. Typically, hydrogen-induced cracking can be controlled by controlling the welding conditions such as the welding environment and pre- and postweld heat treatments. In fact, the preliminary work on the effect of pre- and postweld heat treatments has shown the benefit of these treatments in eliminating cold cracking in FA-129 alloy (Ref. 38). This is being further investigated, and it is the subject of another paper to be published in the near future.

Table 2 — Gas Tungsten Arc Weldability

	Welding Speed, mm/s			
Heat	4.2	8.4	12.7	25.4
FA-122B	C[b]	C[b]	C[a]	C[a]
FA-124B	NC	NC	NC	C[a]
FA-127B	NC	NC	NC	C[a]
FA-129B	NC	NC	NC	C[a]
FA-122BQ	C[b]	C[b]	NC	C[c]
FA-124BQ	NC	NC	NC	C[a]
FA-127BQ	NC	C[a,c]	NC	C[c]
FA-129BQ	NC	NC	NC	C[c]

Note: NC — no Crack; C — crack.
(a) Centerline crack.
(b) Full-length centerline crack.
(c) Transverse crack

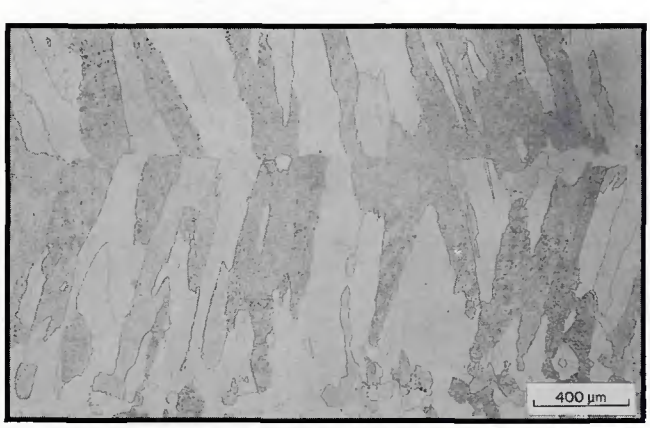

A

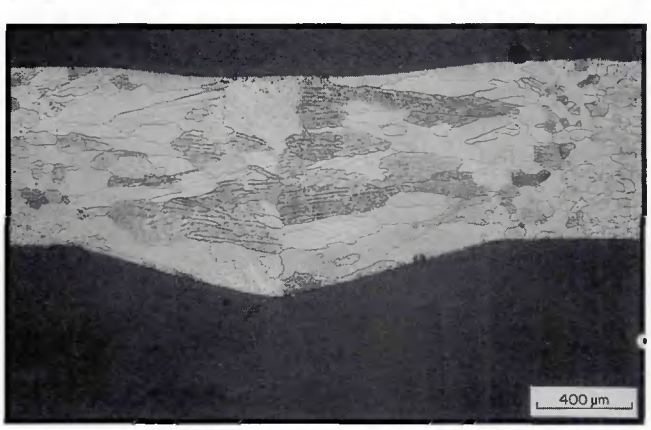

B

Fig. 7 — Optical photomicrographs. A — Surface; B — transverse sections of FA-129B gas tungsten arc weld (25.4 mm/s).

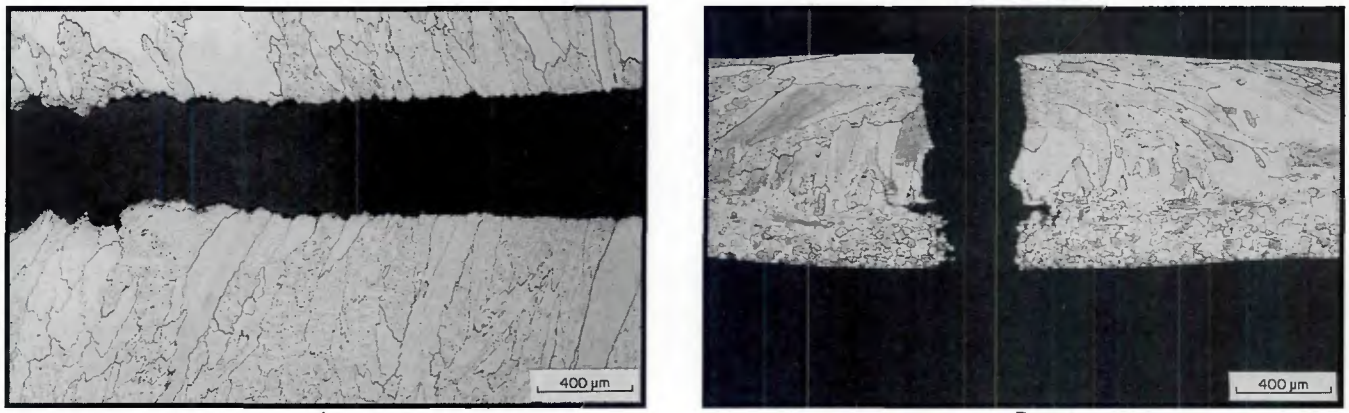

A B

Fig. 8 — Optical photomicrographs. A — Surface; B — transverse sections of FA-122B gas tungsten arc weld (25.4 mm/s) containing centerline crack.

Sigmajig Testing

The susceptibility to FZ solidification cracking and HAZ cracking may be established using any one of several conventional hot-cracking tests (Ref. 39). Susceptibility of iron aluminide to hot cracking was investigated using the Sigmajig test (Ref. 26). In the Sigmajig test, an indicator that is used to determine the susceptibility to FZ cracking is the threshold stress σ_0 above which cracking first occurs during welding. Based on the preliminary melt run experiments of the various alloys, only two alloys, FA-127B and FA-129B, were selected for Sigmajig test evaluation. The test results are summarized and compared with other aluminides as shown in Fig. 12. The measured σ_0 for FA-127B and FA-129B were 20 ksi (137 MPa) and 25 ksi (172 MPa), respectively. Of these two alloys, FA-129B seems to be a promising alloy for further evaluation. The minimum threshold stress value of 25 ksi for FA-129B is within the material range of austenitic stainless steels and some other aluminides as shown in Fig. 12.

Summary

The weldability of a series of Fe_3Al alloys was investigated. The results indicate that, in general, successful welds without cracking can be produced in these alloys using the electron beam process. This was attributed to the highly concentrated heat source and possible refinement of the microstructure. On the other hand, GTA welds revealed a cracking tendency in all of the alloys considered except FA-129B. Alloy FA-122B containing zirconium and boron cracked severely during GTA welding. Evaluation of hot-cracking susceptibility indicates that these alloys are sensitive to minor changes in compositions. Cracking susceptibility in these alloys was found to be very sensitive to the additions of boron and zirconium. Further investigations of Alloy FA-129B using the Sigmajig weldability test revealed that this alloy is not susceptible to hot cracking. The minimum threshold stress of 25 ksi measured for FA-129B is within the material range of some commercial stainless steels. Alloy FA-129BQ has shown some tendency for delayed cold cracking. Work on environmental embrittlement has shown that hydrogen is the embrittling agent in these alloys.

Acknowledgments

The authors acknowledge the assistance of R. W. Reed for his preparation of the specimens. They also thank G. M. Goodwin and C. G. McKamey for reviewing the manuscript, K. Gardner, for preparing the manuscript, and K. Spence for editing. This research was sponsored by the Fossil Energy Advanced Research and Technology Development (AR&TD) Materials Program, U.S. Department of Energy, under contract DE-AC05-840R21400 with Martin Marietta Energy Systems, Inc.

References

1. Stoloff, N. S., and Davies, R. G. 1966. The mechanical properties of ordered alloys. *Prog. Mater. Sci.* 13(1):1.

2. Kear, B. H., Sims, C. T., Stoloff, N. S., and Westbrook, J. H. 1970. Ordered alloys-structural applications and physical metal-

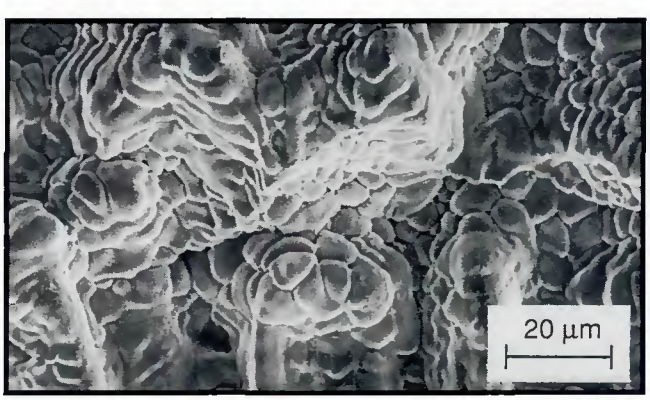

Fig. 9 — 5canning electron micrograph of FA-122B weld centerline crack surface showing dendritic features typical of a hot crack.

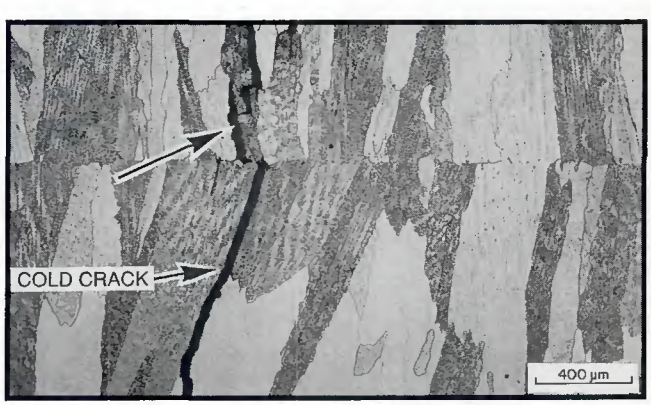

Fig. 10 — Optical photomicrographs of delayed cold crack in FA-129BQ gas tungsten arc weld.

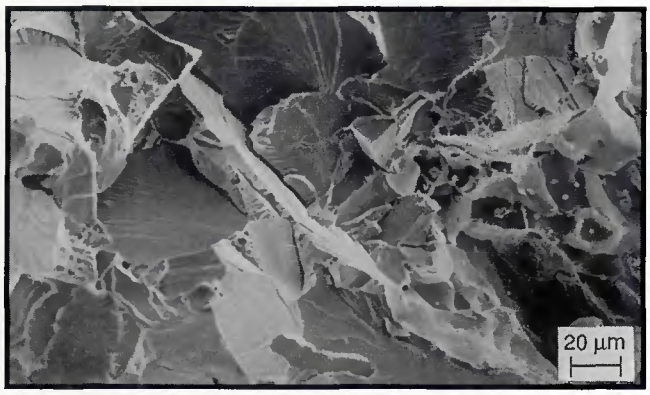

Fig. 11 — Scanning electron micrograph of a typical cold-cracked surface of FA-129BQ alloy weldment.

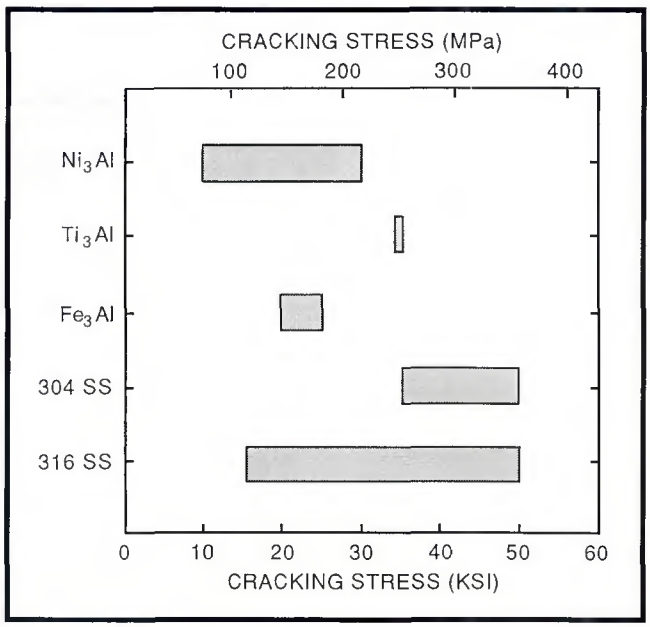

Fig. 12 — Histrogram summary of Sigmajig test results.

lurgy. *Proceedings of the 3rd Bolton Landing Conference*, Claitors, Baton Rouge, La.

3. Westbrook, J. H. 1959. *Mechanical Properties of Intermetallic Compounds*. Wiley, New York, N.Y.

4. Westbrook, J. H. 1967. *Intermetallic Compounds*. Wiley, New York, N.Y.

5. Lipsitt, H. A. 1985. Titanium aluminides – an overview. *High Temperature Ordered Intermetallic Alloys*, Mater. Res. Soc. Symp. Proc., Vol. 39, p. 351.

6. Liu, C. T. 1984. Physical metallurgy and mechanical properties of ductile ordered alloys (Fe, Co, Ni_3V). *Int. Metall. Rev.* 29:168.

7. Stoloff, N. S. 1989. Physical and mechanical metallurgy of Ni_3Al and its alloys. *Int. Mater. Rev.* 34:153.

8. Johnston, T. L., Davies, R. G., and Stoloff, N. S. 1965. Slip character and the ductile-to-brittle transition of single phase solids. *Philos. Mag.* 12:305.

9. Seybolt, A. U., and Westbrook, J. H. 1964. Oxygen induced grain boundary hardening in NiGa. *Acta Metall*. 12:449.

10. Westbrook, J. H., and Wood, D. L. 1962–1963. *J. Inst. Met.* 91:174.

11. Rhodes, C. G., Hamilton, C. H., and Paton, N. E. 1987. Titanium aluminides for elevated temperature applications. *AFML-TR-78-130*.

12. Strychor, R., Williams, J. C., and Soffa, W. A. 1988. Phase transformations and modulated microstructures in Ti-Al-Nb alloys. *Metall. Trans. A.* 19A: 225.

13. David, S. A., and Santella, M. L. 1990. Welding behavior and welding metallurgy of ductile intermetallic alloys. *Advances in Welding Metallurgy*, Proceedings of the First United States-Japan Symposium, American Welding Society, Miami, Florida, p. 65.

14. David, S. A., Jemian, W. A., Liu, C. T., and Horton, J. A. 1985. Welding and weldability of nickel-iron aluminides. *Welding Journal* 64(1):22-s.

15. Santella, M. L., and David, S. A. 1986. Weldability of Ni_3Al type aluminide alloys. *Welding Journal* 65(5):129-s.

16. David, S. A., Horton, J. A., McKamey, C. G., Zacharia, T., and Reed, R. W. 1989. Welding of Iron Aluminides. *Welding Journal* 68(9):372-s.

17. David, S. A., Braski, D. N., and Liu, C. T. 1986. Structure and properties of welded long-range-ordered alloys. *Welding Journal* 65(4):93-s.

18. Ziegler, N. 1932. Resistance of iron-aluminum alloys to oxidation at high temperatures. *AIME Trans.* 100:267.

19. Sykes, C., and Bampfylde, J. 1934. The physical properties of iron-aluminum alloys. *J. Iron and Steel Inst.* 130:389.

20. Bordeau, R. G. 1987. Development of iron aluminides. AFWAL-TR-87-4009, Air Force Wright Aeronautical Laboratories, Wright-Patterson Air Force Base, Dayton, Ohio.

21. Culbertson, G., and Kortovich, C. S. 1986. Development of iron aluminides. AFWAL-TR-85-4155, Air Force Wright Aeronautical Laboratories, Wright Patterson Air Force Base, Dayton, Ohio.

22. Sikka, V. K., McKamey, C. C., Howell, C. R., and Baldwin, R. H. 1990. Fabrication and mechanical properties of FeAl-based aluminides. ORNL/TM-11465, Martin Marietta Energy Systems, Inc., Oak Ridge National Laboratory, Oak Ridge, Tenn.

23. McKamey, C. G. 1990. Development of iron aluminides. Proceedings of the Fourth Annual Conference on Fossil Energy Materials, ORNL/FMP-90/1, U.S. Department of Energy, Oak Ridge, Tenn.

24. McKamey, C. G., DeVan, J. H., Tortorelli, P. F., and Sikka, V. K. 1991. A review of recent developments in Fe_3Al-based alloys. *J. Mater. Res.* 6(8): 1779.

25. McKamey, C. G., Liu, C. T., David, S. A., Horton, J. H., Pierce, D. H., and Campbell, J. J. 1988. Development of iron aluminides for coal conversion systems. ORNL/TM-10793, Martin Marietta Energy Systems, Inc., Oak Ridge National Laboratory, Oak Ridge, Tenn.

26. Goodwin, G. M. 1987. Development of a New Hot-Cracking Test — Sigmajig. *Welding Journal* 77(2):33-s.

27. Puzak, P. P., Apblett, W. R., and Pellini, W. S. 1956. Hot cracking of stainless steel weldments. *Welding Journal* 35(1):96-s.

28. Apblett, W. R., and Pellini, W. S. 1954. Factors which influence weld hot cracking. *Welding Journal* 33(2):83-s.

29. Borland, J. C. 1960. Hot cracking in welds. *Br. Weld. J.* 7:558–559.

30. Hull, F. C. 1967. Effects of delta ferrite on the hot cracking of stainless steel. *Welding Journal* 46(9):399-s.

31. Vero, J. 1936. *Met. Ind.* (London) 48:431–437.

32. Singer, A. R. E. and Jennings, P. H. 1946. Properties of the Al-Si 1035 Alloys at temperatures in the region of the solidus. *J. Inst. Met.* 73:33–54.

33. Singer, A. R. E. and Jennings, P. H. 1947. Hot-shortness of some high purity alloys. *J. Inst. Met.* 74:227-40.

34. Pellini, W. S. 1952, Strain theory of hot tearing. *Foundry* 80: 124–33.

35. Borland, J. C. 1960. Generalized theory of super solidus cracking in welds and castings. *Br. Weld. J.* 7:508-512.

36. Smith, C. S. 1948. Grains, phases and interfaces. *Trans. of the AIME*, 175:15–51.

37. Liu, C. T., McKamey, C. G., and Lee, E. H. 1990. Environmental effects on room-temperature ductility and fracture in Fe_3Al. *Scr. Metall*. 24:385-90.

38. Zacharia, T., and David, S. A. 1992. unpublished data, Martin Marietta Energy Systems, Inc., Oak Ridge National Laboratory, Oak Ridge, Tenn.

39. Vagi, J. J., Meister, R. P., and Randall, M. D. 1958. Weldment evaluation methods. DMIC-244, Columbus, Ohio.